YMTHE, Volume *29*

Supplemental Information

TV-circRGPD6 Nanoparticle Suppresses Breast Cancer Stem Cell-Mediated Metastasis via the miR-26b/YAF2 Axis

Xiaoti Lin, Weiyu Chen, Fengqin Wei, and Xiaoming Xie

SUPPLEMENTAL INFORMATION

Supplemental Experimental Procedures

Supplementary Tables S1-4

Supplementary Figures S1-7

Supplemental Experimental Procedures

Patients and animal studies

Informed consent was obtained from all patients. All animal experiments and related studies were approved by the research ethics committee of Sun Yat-sen University Cancer Center (SYSUCC).

Cell culture and transfection procedure of breast cancer stem cells (BCSC)

Tumor tissue-derived BCSC (XM322 and XM607) were isolated by fluorescence-activated cell sorting (FACS) as previously described. [1] Cell line-derived BCSC (MDA-MB-231.SC and MCF-7.SC) were purified by magnetic-activated cell sorting (MACS). [2] The application of culture medium was as described previously. BCSC were maintained as spheres in ultralow attachment flasks in serum-free DMEM-F12 and supplemented with 10 ng/mL basic fibroblast growth factor (BFGF), 20 ng/mL epidermal growth factor (EGF), 2% B27, 5 μg/mL insulin, and 10000 IU/mL penicillin-streptomycin. BCSC were maintained as spheres in ultralow attachment flasks in serum-free DMEM-F12 and supplemented with 10 ng/mL basic fibroblast growth factor (BFGF), 20 ng/mL epidermal growth factor (EGF), 2% B27, 5 μg/mL insulin, and 10000 IU/mL penicillin-streptomycin. For preparing of single cell suspensions, BCSC were digested by TrypLE™ Express for 9 min. To establish adherent cells in differentiation culture, we added 0.50% bovine serum albumin to nutrient solution for 12 days.

MDA-MB-231, MCF-7, MDA-MB-468 and SK-br-3 breast cancer cell lines, and immortalized normal mammary epithelial cell lines (MCF-12A, 184A1) were all purchased from American Type Culture Collection (ATCC). All cell lines were cultured according to the vendor’s instructions. Briefly, the breast cancer cells were maintained under DMEM medium supplemen-ted with 10% fetal bovine serum (FBS, GIBCO, Campinas, Brazil). Immortalized normal mammary epithelial cells were raised under Mammary Epithelium Basal Medium (Clonetics, Walkersville, MD). All cells were bred at 37°C in a 5% CO_2 incubator.

Cholesterol and 1, 2-bis(oleoyloxy)-3-(trimethyl ammonio) propane (DOTAP; Avanti Polar Lipids, Alabaster, AL), were extruded and DOTAP: cholesterol liposomes were performed according to the protocol. Briefly, to evaluate the

inhibitory effects on BCSC, the cells were transiently cotransfected in 24-well plates with 1mg of the TV plasmid DNA plus 0.1mg of CMV-Luc DNA using extruded DOTAP:cholesterol liposomes at an N/P ratio of 2:1 secons.

Patients, tissues, tissue microarray construction (TMA), immunohistochemistry (IHC) and *in situ* hybridization (ISH)

A total of 1691 female patients with breast cancer who hospitalized in SYSUCC from October 2001 to September 2013 were enrolled in our study. A complete patient follow-up was performed, and endpoint of this follow-up was August 2017. Expression data were obtained from 248 fresh-frozen resected breast specimens consisting of 165 tumor tissues and 83 adjacent normal breast tissues. Antibodies of YAF2 (1: 100) was performed. A total of 12 mouse tissues were involved in analyzing of IHC expressions. The primary antibodies included ER (1:50), PR (1:500), HER2 (1:50), Ki-67 (1:100), E-Cadherin (1:100), α-SMA (1:200), and Muc1 (1:50). The circRGPD6 detection probe was used for *in situ* hybridization (ISH) according to manufacturer's protocol (Exiqon, Vedbaek, Denmark). In addition, staining procedures were performed by using Bench Mark XT automated IHC/ISH slide staining system.

Protocols of fluorescence in situ hybridization (FISH) were as follow. Briefly, hybridization was performed overnight with circRGPD6 probes. Specimens were analyzed using a Nikon inverted fluorescence microscope. The circRGPD6 probe for FISH is 5′-TTGAAGCCAGGTAGTGAAAG-3′. This assay was repeated three times.

We graded IHC/ISH status based on the combination synthetical evaluation of quantity and intensity of positive cells. Briefly, staining intensity index was grouped into four grades: negative-0 point, weak-1 point, moderate-2 points, and strong-3 points. Percentage of positive cells was segmented into 5 ranks: 0 point (0%), 1 point (1% ~ 24%), 2 points (25% ~ 49%), 3 points (50% ~ 74%), and 4 points (75% ~ 100%). The total score of both determined the status of YAF2 expression: negative (0 ~ 3 points) and positive (≥ 4 points).

In addition, we randomly analyzed of circRGPD6 expression in 22 clinical samples with breast cancer and their adjacent healthy breast tissue samples. The specimens obtained from female patients who hospitalized in SYSUCC from January

2015 to May 2015.

RNA isolation and quantitative RT-PCR (qRT-PCR)

Total RNA was extracted from flash-frozen tissue samples or cultured cells using TRIzol Reagent (Invitrogen), according to the manufacturer's instructions. For RNA retro-transcription, the SuperScript VILO cDNA Synthesis Kit was performed (Thermo Fisher Scientific). For the detection of circRNAs and their linear counterparts, cDNA samples were analysed by quantitative real-time PCR using PowerUp SYBR Green Master Mix (Thermo Fisher Scientific). For the RNA extracted in CLIP experiments, quantitative real-time PCR was performed on cDNAs using MyTaq Red DNA Polymerase (Bioline) according to the manufacturer's instructions. The samples were then loaded on a 2.5% agarose gel. All the images were captured using the Molecular Imager ChemiDoc XRS + (Bio-Rad), and the densitometric analyses were performed using the associated Image Lab software (Bio-Rad). Each sample was analyzed at least in triplicate.

Reverse transcription PCR

Reverse transcription for mRNA and circRNAs was performed with an MMLV-RT kit (Takara, Mountain View, CA) using random hexamers according to the manufacturer's protocols. PCR was subsequently performed with a 1:10 dilution of reverse-transcribed cDNA. The PCR product was run in a 2% agarose gel. Quantitative real-time reverse transcription polymerase chain reactions were performed on a 7500 Real-time PCR System (Applied Biosystems, Carlsbad, CA, USA) with Universal SYBR Green Master Mix (4,913,914,001, Roche, Shanghai, China). Meanwhile, we used 18s rRNA as the internal references for circRNA.

Pull down assay

A total of 1×10^7 BCSC were harvested, lysed and sonicated. The TV-circRGPD6 probe was used for incubation with C-1 magnetic beads (Life Technologies) at 25 °C for 2 hr to generate probe-coated beads. Cell lysate with TV-circRGPD6 probe or oligo probe was incubated at 4 °C for one night. After washing with wash buffer, the RNA mix bound to the beads was eluted and extracted with an RNeasy Mini Kit (QIAGEN) for RT–PCR or real-time PCR.

Oligonucleotide transfection

The human breast cell lines MCF-7.SC and XM322 were seeded in a 6-well plate and incubated at 37 °C in humidified 5% CO2 atmosphere overnight. CircRGPD6 siRNA, miRNA mimics and inhibitors (RiboBio, Guangzhou, China) were transfected by Lipofectamine RNAiMax (Life Technologies) according to the manufacturer's protocol.

Northern blot analysis

Digoxin-labeled DNA probes (351 nt), spanning the back-splice junction of circRGPD6, were prepared from cDNA using PCR DIG Probe Synthesis Kit (Roche, Mannheim, Germany). Total RNA (10 μg) denatured in formaldehyde was resolved on 1% agarose-formaldehyde gel and transferred onto a Hybond-N+ nylon membrane (Buckinghamshire, UK). Membranes were crosslinked, pre-hybridized in DIG Easy Hyb (Roche), following hybridized with DIG-labeled DNA probes overnight. After stringent washing, the membranes were incubated with alkaline phosphatase (AP)-conjugated anti-DIG antibodies (Roche). Immunoreactive bands were visualized using chemiluminescent substrate CSPD (Roche) followed by exposure to X-ray film.

Clonal pair-cell analysis

In brief, MCF-7.SC and XM322 (5×10^6) cells were transfected with GFP-labeled TV-circRGPD6 plasmid for 48 h, stained with 2 μL DAPI (10 μg/mL) for 5 min, and counterstained with anti-CD44-PE (1:200) for 30 min, respectively. Initially, GFP-labeled BCSC were purified and collected. Next, images were acquired by an inverted epifluorescence microscope system and further analyzed by digital confocal microscopy. Similarly, while we evaluated the association of loss of CD44 and p-H2AX expression in BCSC, clonal pair-cell analysis was performed. In brief, MCF-7.SC and XM322 (5×10^6) cells were transfected with GFP-labeled p-H2AX plasmid for 48 h, stained with 2 μL DAPI (10 μg/mL) for 5 min, and counterstained with anti-CD44-PE (1:200) for 30 min, respectively. Preliminarily, GFP-labeled BCSC were purified and collected. Next, images were acquired by an inverted epifluorescence microscope system and further analyzed by digital confocal microscopy.

Western blot analysis

Protein extracts of BCSC (10μg protein) were detached by 10 % SDS-PAGE and

electrophoretically transferred to polyvinylidene difluoride (PVDF) membrane. Following, antibodies were assayed. Antibodies of CD44, Vimentin, E-cadherin, N-cadherin, HIF-1α and YAF2 were purchased from Cell Signaling Technology. We performed GAPDH as internal control. Signals were visualized using the Supersignal West Pico ECL chemiluminescence detection kit and Kodak X-ray film.

Flow cytometry

Fluorescence-activated cell sorting (FACS) was performed to determine the $CD44^{+}CD24^{-}$ subpopulation, and proportion of Lin or ALDH1 in BCSC by using $CD44^{+}$, $CD24^{-}$, Lin-PE and ALDH1-PE antibodies (Sigma). To develop adherent cells in differentiation culture, we added 0.50% bovine serum albumin to nutrient solution for 12 days. Differentiation capabilities of BCSC were further analyzed by flow cytometry. Briefly, BCSC (5×10^{7} cells) were incubated with Muc1-PE or α-SMA-PE antibody for 48 hr (Sigma). Positive GFP-labeled cells were purified by FACS. Then, isolated cells were contained with 2 μl DAPI (10 μg/mL) for 5 min. We used CellQuest software to analyze the data.

Clonogenicity assays in soft agarose

Clonal expansion ability of BCSC was analyzed by clonogenicity assays in soft agarose. Briefly, BCSC were transfected with Negative Ctrl (NC) plus miR-Ctrl, TV-circRGPD6 plus miR-Ctrl, NC plus miR-26b and TV-circRGPD6 plus miR-26b, respectively. Next, 2% solidified agar was paved as base agar in 6-well. BCSC were seeded at 3×10^{3} cells per well coated with a thin layer of 1% soft agarose. The experiment was terminated at day 21, and wells were Giemsa-stained. Spheres with 50 μm or greater in diameter were determined. We performed all experiments for three times.

Establishment of serial passages of luciferase-labeled and green fluorescent protein (GFP)-labeled BCSC lineages

Protocol of serial passages of cell lines expressing firefly luciferase was previously described.[1-3] Briefly, BCSC were transfected with pEF1a-Luc-Neo, and filtrated with G418 for 14 days. Next, G418-resistant clones, referred as luciferase-labeled BCSC, were collected and maintained for further *in vivo* experiments. Similarly, BCSC were transfected with pcDNA3.1-EGFP-NEO plasmid. Then GFP-labeled BCSC were

selected out with G418 for 14 days. Following, GFP expression and survival BCSC were cultured. Here, G418-resistant clones were designated as GFP-labeled BCSC.

Determination of synergistic effects of TV-circRGPD6 and docetaxel

GFP-labeled BCSC were transfected with Ctrl, TV-circRGPD6, si-circRGPD6, docetaxe, as well as TV-circRGPD6 plus docetaxel. We used a spinning disk confocal long-term live cell imaging system (Olympus CV1000) to maintain and photograph these cells in real time. Mammospheres with 50 μm or greater in diameter were determined. For the detection of synergistic effects of TV-circRGPD6 and docetaxel, BCSC were treated with Ctrl, 2 nM docetaxel (Aventis Pharma, France), [4] presence or absence of docetaxel after 0.1 nM TV-circRGPD6 transduction during in the corresponding period (0 day, 1 day, 3 days and 5 days) respectively. GFP intensity was measured with MetaMorph image acquisition and analysis software (Molecular Devices). All experiments were repeated for five times.

MTT assay of cell proliferation

MTT (Sigma) assay was used to assess MCF-7.SC cell viability according to the manufacturer's instructions. Each assay was repeated five times.

Terminal deoxynucleotidyl transferase-mediated dUTP nick-end labeling (TUNEL) test

TUNEL staining for apoptosis was performed using the ApopTag Plus Peroxidase In Situ Apoptosis Detection kit (Invitrogen CA, USA) according to the manufacturer's instructions.

Constructs and transfection

Detailed information of the VISA plasmid, hTERT promoter-driven VISA nanoparticle delivery of circRGPD6 (TV-circRGPD6) were described previously. [1-3, 5-7] Briefly, the circRGPD6 shRNA was incorporated into the Bgl II/Nhe I sites of the plasmid pGL3-T-VISA-Luc; following, the T-VISA-circRGPD6 fragment of pGL3-T-VISA-circRGPD6 was subcloned into the Not I and Sal I sites of pUK21. Transient transfections were performed as previously described. [1, 2] Briefly, BCSC were transiently transfected with 1μg of the hTERT-VISA plasmid DNA using extruded DOTAP: cholesterol liposomes in 24-well plates (N/P ratio of 2:1). Silence sequence of circRGPD6: GTTGCTCAAGAGCCTCCATTA. For site-specific

mutagenesis, we mutated the regions in the circRGPD6-3'UTR and YAF2-3'UTR complementary to the seed sequence of miR-26b using the QuikChange II Site-Directed Mutagenesis Kit according to manufacturer's protocol.

In the evaluation of the effect of circRGPD6/miR-26b/YAF2 axis on mammosphere formation of BCSC, both MCF-7.SC and XM322 were transfected with Ctrl, TV-circRGPD6, miR-26b, miR-26b plus TV-circRGPD6, miR-26b plus YAF2 3'UTR, and miR-26b plus YAF2 3'UTR-mut-both. We used a spinning disk confocal long-term live cell imaging system (Olympus CV1000) to maintain and photograph these cells in real time. Mammospheres with 50 μm or greater in diameter were determined. All experiments were repeated for three times.

Tumor transplantation experiments

To identify the stem-like properties of metastatic breast cancer cells, we generated orthotopic xenograft models of breast cancer MCF-7 cells. In total, MCF-7 cells were maintained in 12 athymic female non-obese diabetic/severe combined immunodeficient (NOD/SCID) mice to produce both primary tumor and dissemination for 4 weeks. Following, the stem-like properties of primary tumors were compared with their corresponding disseminated tumors.

To test early dissemination capabilities of MCF-7 *in vivo*, we generated orthotopic xenograft models of luciferase-labeled MCF-7 and their luciferase-labeled primary breast cancer cell-bearing. The details were described previously. [1-3, 5, 6, 8] Briefly, NOD/SCID mice were injected subcutaneously into the left fourth mammary gland with 1×10^5 cells primary breast cancer cells or MCF-7 using a 25-gauge needle (n = 9 mice per group). After transplantation, mice were monitored using the *In Vivo* Imaging System (*IVIS*, Xenogen, Alameda, CA) to early dissemination for 10 days. All the mice were then sacrificed and tissue was collected to characterize the capability of tumor formation.

To determine BCSC mediate breast cancer metastasis, ten luciferase-labeled BCSC-bearing mice were maintained (MCF-7.SC and XM322, 5 mice per group). All of mammosphere formation, self-renewal capacity, $CD44^+CD24^-Lin^{-/low}ALDH1^+$ expressions and pluripotency capability of early disseminated tumors in the above-mentioned 10 mice were analyzed.

With a goal of exploring the potential synergy effect of TV-circRGPD6 plasmid and docetaxel in eradicating metastasis of breast cancer cells *in vivo*, a suspension of XM322-luciferase cells (5×10^6) was inoculated at the left fourth inguinal mammary gland of NOD/SCID mice using a 30-gauge needle. Tumor formation was monitored by palpation and tumor size was measured twice per week using calipers. We developed and maintained XM322 lineages with expression of firefly luciferase for 40 days (Day 0). When the tumors developed metastatic tumors with nonsignificant expressions of firefly luciferase, the mice were noninvasively imaged using the *IVIS* In Vivo Imaging System (Xenogen, Alameda, CA) to confirm tumor growth and then randomly assigned to one of five treatment groups (n = 3 mice per group). Each group of mice received 100 μL of DNA-liposome complexes that contained liposomal (Ctrl) alone, si-circRGPD6 liposomal complexes (10 μg qod), TV-circRGPD6 liposomal complexes (10 μg qod), doxetaxel (10 mg/kg qod for 5 times) alone, and TV-circRGPD6 liposomal complexes (10 μg qod) plus doxetaxel (10 mg/kg qod for 5 times), respectively. Tumor progression was monitored daily using the IVIS system. The luciferase test was performed for the following 20 days (Day 20) investigation and then the data were analyzed. Fine needle aspirations on mice were done according to standard cytopathologic practice under inhaled general anesthesia (isofluorane) using 10-mL syringes and 25-gauge needles. Fine needle aspirations were done at baseline for all mice and after 20 days of therapy for each of the primary tumors, disseminated tumor and disseminated tumor. Quantitative RT-PCR of circRGPD6 expression, FACS analysis $CD44^+CD24^-$ subpopulation and determination of firefly luciferase of BCSC-bearing tumors were performed according to manufacturer's protocol. Each experiment was repeated more than three times.

To evaluate the safety conditions of circRGPD6 treatment to BCSC *in vivo*, a suspension of XM322 cells (1×10^4) was inoculated at the left fourth inguinal mammary gland of NOD/SCID mice. When the tumors reached to ~50 mm^3, the mice were non-invasively imaged using the *In Vivo* Imaging System (IVIS, Xenogen, Alameda, CA) to monitor tumor growth. Then, all mice were randomly divided into three treatment groups (10 mice per group). Each group of mice received 100 μL of DNA-liposome complexes that contained TV-circRGPD6 liposomal complexes (10 μg qod), si-circRGPD6 liposomal complexes (10 μg qod) or liposomal (Ctrl) alone. The secretion levels of serum alanine transaminase (ALT), aspartate transaminase

(AST), blood urea nitrogen (BUN) and creatinine (Cr) were determined with an automatic analyzer (Roche Cobas Mira Plus; Roche, Mannheim, Germany). Mouse serum cytokines (TNF-α, IL-6 and IFN-γ) were quantified using the cytometric bead array kit (CBA; BD Biosciences). The test was repeated more than five times.

We performed *in vivo* experiments to determine the ability of TV-circRGPD6 inhibiting stem-like biological properties of metastatic breast cancer. In the beginning, NOD/SCID nude mice were injected subcutaneously into the right fourth mammary gland with 5×10^6 either immortal healthy mammary epithelial 184A1 cells, primary XM322 breast cancer cells in 100ml PBS using a 30-gauge needle. Mice were monitored twice a week, tumor formation was monitored by palpation and tumor size value was measured in cubic millimeters using calipers. Tumor volume was calculated using the standard formula: tumor volume = (width^2 × length ×π)/6. When the tumors size reached to ~50 mm^3, the mice were randomly assigned to the five treatment groups (3 mice per group): liposomal (Ctrl) alone, si-circRGPD6 liposomal complexes (10 μg qod), TV-circRGPD6 liposomal complexes (10 μg qod), doxetaxel (10 mg/kg qod for 5 times), [9] and TV-circRGPD6 liposomal complexes (10 μg qod) plus doxetaxel (10 mg/kg qod for 5 times), respectively. Similarly, a suspension of XM322-luciferase cells (1×10^4) was inoculated at the left fourth inguinal mammary gland of NOD/SCID mice. We selected out mice with tumor dissemination and the tumor photon signals reached to ~500×10^6 photons/second for the following 20 days intervention.

Microarray analyses of mRNA expression profiles

RNA-Seq and microarray analyses were performed on BCSC transfected with TV-circRGPD6 and si-circRGPD6 for 48 hr. RNA extractions were performed using Trizol. Synthesis of cDNA was performed using the SuperScript Choice System according to manufacturer's protocol (Invitrogen Life Technologies, Capital Biochip Corporation). Microarrays analyses were performed using Affymetrix Genechip scanner 3000 with Affymetrix Genechip Command Console software. Microarray experiments were conducted according to the manufacturer's instructions. To select the differentially expressed genes, we used threshold values of ≥ 2 and ≤ -2 -fold change and a Benjamini-Hochberg corrected *p* value of 0.05. Gene expressions were normalized by using Log2 transformation and then median-centering was used for the

adjustment by the Adjust Data function of Cluster 3.0 software. Data was subsequently analyzed for hierarchical clustering with average linkage (genes which value more than 100 were evaluated). Finally, we performed tree visualization with Java Treeview (Stanford University School of Medicine, Stanford, CA, USA). The results had been submitted to ArrayExpress (accession number E-MTAB-5584, E-MTAB-7556 and E-MTAB-7557).

REFERENCES

1. Lin X, Chen W, Wei F, Zhou BP, Hung MC, Xie X. (2017) POMC maintains tumor-initiating properties of tumor tissue-derived long-term-cultured breast cancer stem cells. Int. J. Cancer *140*, 2517-2525.
2. Lin X, Chen W, Wei F, Zhou BP, Hung MC, Xie X. (2017) Nanoparticle Delivery of miR-34a Eradicates Long-term-cultured Breast Cancer Stem Cells via Targeting C22ORF28 Directly. Theranostics *7*, 4805-4824.
3. Xie X, Xia W, Li Z, Kuo HP, Liu Y, Li Z, et al. (2007) Targeted expression of BikDD eradicates pancreatic tumors in noninvasive imaging models. Cancer Cell *12*, 52-65.
4. Merino D, Whittle J, Vaillant F, Serrano A, Gong JN, Giner G, et al. (2017) Synergistic action of the MCL-1 inhibitor S63845 with current therapies in preclinical models of triple-negative and HER2-amplified breast cancer. Sci. Transl. Med. *9*, 7049-7059.
5. Lang JY, Hsu JL, Meric-Bernstam F, Chang CJ, Wang Q, Bao Y, et al. (2011) BikDD eliminates breast cancer initiating cells and synergizes with lapatinib for breast cancer treatment. Cancer Cell *20*, 341-356.
6. Li L, Xie X, Luo J, Liu M, Xi S, Guo J, et al. (2012) Targeted expression of miR-34a using the T-VISA system suppresses breast cancer cell growth and invasion. Mol. Ther. *20*, 2326-2334.
7. Huang HC, Pigula M, Fang Y, Hasan T. (2018) Immobilization of Photo-Immunoconjugates on Nanoparticles Leads to Enhanced Light-Activated Biological Effects. Small *1*, e1800236.
8. Xie X, Li L, Xiao X, Guo J, Kong Y, Wu M, et al. (2012) Targeted expression of BikDD eliminates breast cancer with virtually no toxicity in noninvasive imaging models. Mol. Cancer Ther. *11*, 1915-1924.
9. Lu Y, Yue Z, Xie J, Wang W, Zhu H, Zhang E, et al. (2018) Micelles with ultralow critical micelle concentration as carriers for drug delivery. Nat. Biomed. Eng. *2*, 318-325.

Supplementary Tables S1-4

Supplementary Table S1. starBase predicts the miRNAs sponging circRGPD6

MiRNA ID	MiRNA Name	Gene ID	Ggene Name	Gene Type	Chromosome	Target Sites
MIMAT0000101	hsa-miR-103a-3p	NM_001037866	RGPD6	circRNA	chr2	8
MIMAT0000104	hsa-miR-107	NM_001037866	RGPD6	circRNA	chr2	8
MIMAT0000423	hsa-miR-125b-5p	NM_001037866	RGPD6	circRNA	chr2	6
MIMAT0000417	hsa-miR-15b-5p	NM_001037866	RGPD6	circRNA	chr2	11
MIMAT0000076	hsa-miR-21-5p	NM_001037866	RGPD6	circRNA	chr2	5
MIMAT0000418	hsa-miR-23b-3p	NM_001037866	RGPD6	circRNA	chr2	9
MIMAT0000080	hsa-miR-24-3p	NM_001037866	RGPD6	circRNA	chr2	9
MIMAT0000083	hsa-miR-26b-5p	NM_001037866	RGPD6	circRNA	chr2	9
MIMAT0000419	hsa-miR-27b-3p	NM_001037866	RGPD6	circRNA	chr2	10
MIMAT0000086	hsa-miR-29a-3p	NM_001037866	RGPD6	circRNA	chr2	8
MIMAT0000100	hsa-miR-29b-3p	NM_001037866	RGPD6	circRNA	chr2	8

Supplementary Table S2. 12 miroRNA expressions were changed following the regulation of circRGPD6 in both MCF-7.SC and XM322

Name of miRNA	Mature sequence
hsa-miR-103a-3p	TCATAGCCCTGTACAATG
hsa-miR-24-3p	CTGTTCCTGCTGAACTGA
hsa-miR-107	TGATAGCCCTGTACAATGCT
hsa-miR-27a-3p	GCGGAACTTAGCCACTG
hsa-miR-125b-5p	TCACAAGTTAGGGTCTC
hsa-miR-27b-3p	GCAGAACTTAGCCACTGT
hsa-miR-15b-5p	TGTAAACCATGATGTGCTGC
hsa-miR-148b-3p	ACAAAGTTCTGTGATGCAC
hsa-miR-26b-5p	ACCTATCCTGAATTACTTGA
hsa-miR-23b-3p	GGTAATCCCTGGCAATG
hsa-miR-29b-3p	AACACTGATTTCAAATGGTGC
hsa-miR-29a-3p	TAACCGATTTCAGATGGTGC

Supplementary Table S3. Thirty-seven co-target genes of miR-26b based on four algorithms (TargetScan, miRanda, TargetMiner and miRWalk)

4 algorithms	37 co-target genes of miR-26b
TargetScan, MIRDB, TargetMiner and miRWalk	As following: ELAVL2, E2F7, RHOQ, PRKCD, SLC38A2, ADAM9, CREBZF, FAM136A, TMCC1, ULK2, PTP4A1, TMEM2, KPNA6, TET3, CXADR, BLOC1S2, ABHD2, ZBTB18, PLOD2, GNA13, TNRC6B, ZNF608, RCOR1, SFXN1, YAF2, HGF, SLC19A2, RCBTB1, PTEN, GTF2A1, ZNF410, USP9X, SACS, CREBRF, REEP4, MAT2A, USP3.

Supplementary Table S4. Clinicopathological features of 165 patients with breast cancer

	Stage I	Stage II	Stage III	Stage IV
Totality	16	58	60	31
Age (years)				
<50	8	35	39	17
≥50	8	23	21	14
Pathogenetic location				
Left breast	8	30	27	15
Right breast	2	28	33	16
Family history of cancer				
Absence	14	56	55	28
Presence	2	2	5	3
Histological type				
Ductal	13	56	59	30
Lobular	3	2	1	1
Pathological grading				
1	4	13	17	3
2	4	18	17	8
3	8	24	19	16
Undifferentiated	0	3	6	3
Not available	0	0	1	1
ER status				
Negative	8	31	44	20
Positive	8	27	16	11
PR status				
Negative	8	30	42	19
Positive	8	28	18	12
Herb2 status				
Negative	14	48	50	17
Positive	2	10	10	14
Triple-negative breast cancer				
Absence	9	45	29	14
Presence	7	13	31	17
p53 status				
Negative	8	30	19	8
Positive	8	28	41	23

Supplementary Figures 1-7

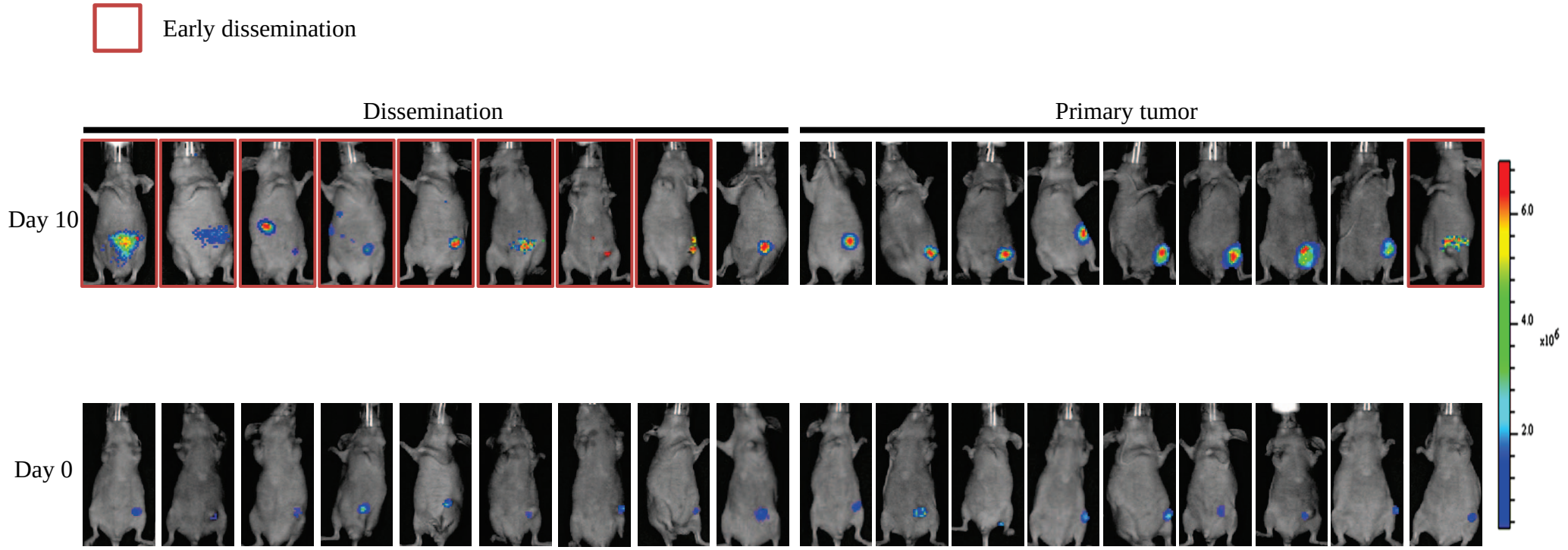

Figure S1. Monitoring dissemination of primary MCF-7-bearing tumor and disseminated MCF-7-bearing tumor in NOD/SCID mice. Mice are imaged for 10 days after implantation when palpable tumors formed.

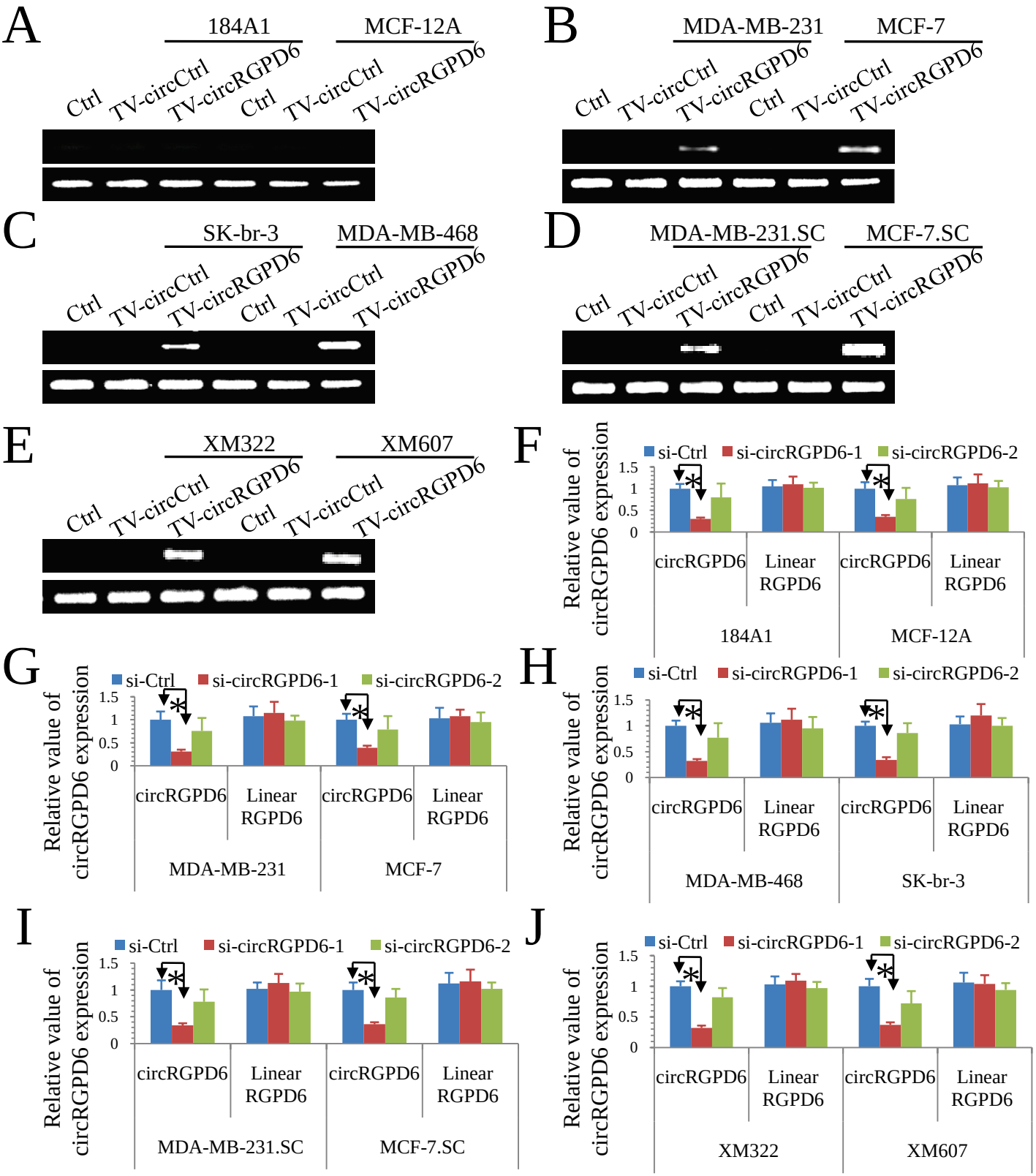

Figure S2. Determination of the regulators of circRGPD6. (A-E) Reverse Transcription-PCR confirmation of circRGPD6 expression in liposomal complex, TV-Ctrl and TV-circRGPD6-transfected breast cells: (A) Healthy mammary epithelial cells: 184A1 and MCF-12A; (B) Breast cancer cells: MDA-MB-231 and MCF-7; (C) Breast cancer cells: SK-br-3 and MDA-MB-468; (D) BCSC lineages derived from breast cancer cells: MDA-MB-231.SC and MCF-7.SC; (E) Tumor tissue-derived BCSC: XM322 and XM607. (F-J) qRT-PCR to verify the circRGPD6 silencing efficiency and rule out the possibility that circ circRGPD6 siRNA might exert effects on the mRNA level of circRGPD6 (linear circRGPD6) in multiple breast cells: (F) 184A1 and MCF-12A; (G) MDA-MB-231 and MCF-7; (H) SK-br-3 and MDA-MB-468; (I) MDA-MB-231.SC and MCF-7.SC; (J) XM322 and XM607. Each experiment was repeated at least in triplicate. * indicates P <0.05. Statistical analysis was performed using the paired t-test.

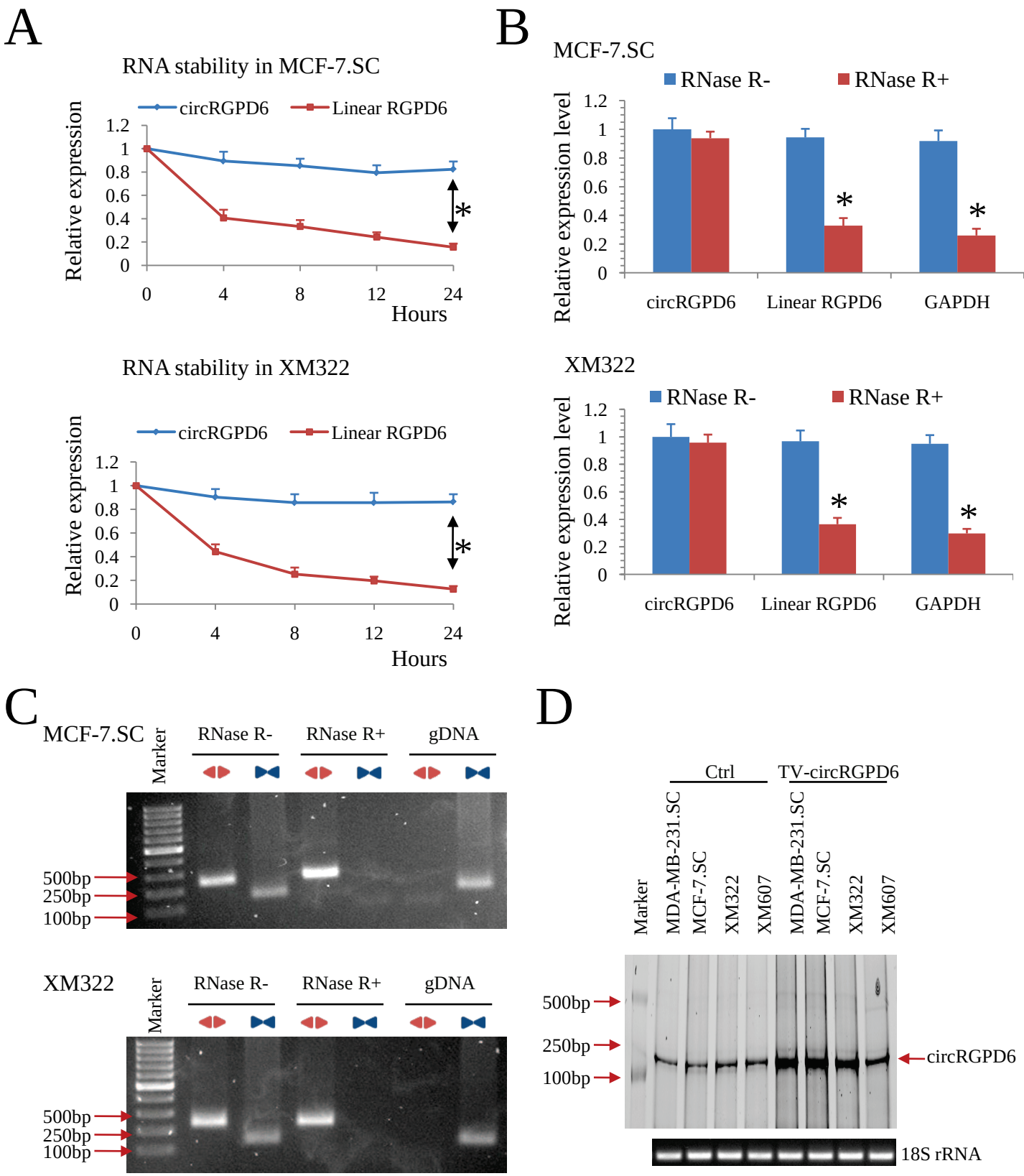

Figure S3. Characteristics of circRGPD6 in BCSC. (A) qRT-PCR for the expression of circRGPD6 and RGPD6 mRNA in both MCF-7.SC and XM322 treated with Actinomycin D, a transcription inhibitor. (B) qRT-PCR assay with specially designed divergent and convergent primers and indicated that circRGPD6, rather than linear RGPD6 or GAPDH, could resist digestion by RNase R. (C) Expression levels of the back-spliced and canonical forms of RGPD6 in the presence or absence of RNase R supplementation in cDNA and gDNA from both MCF-7.SC and XM322 by PCR and an agarose gel electrophoresis assay. (D) Ctrl (empty vector) and TV-circRGPD6 were transfected into BCSC. After 24 hr of transfection, total RNA was treated with RNase-R and subjected to Northern blotting using circRGPD6 junction probes. Each experiment was repeated at least three times. * indicates $P < 0.05$. Statistical analysis was performed using the paired *t*-test.

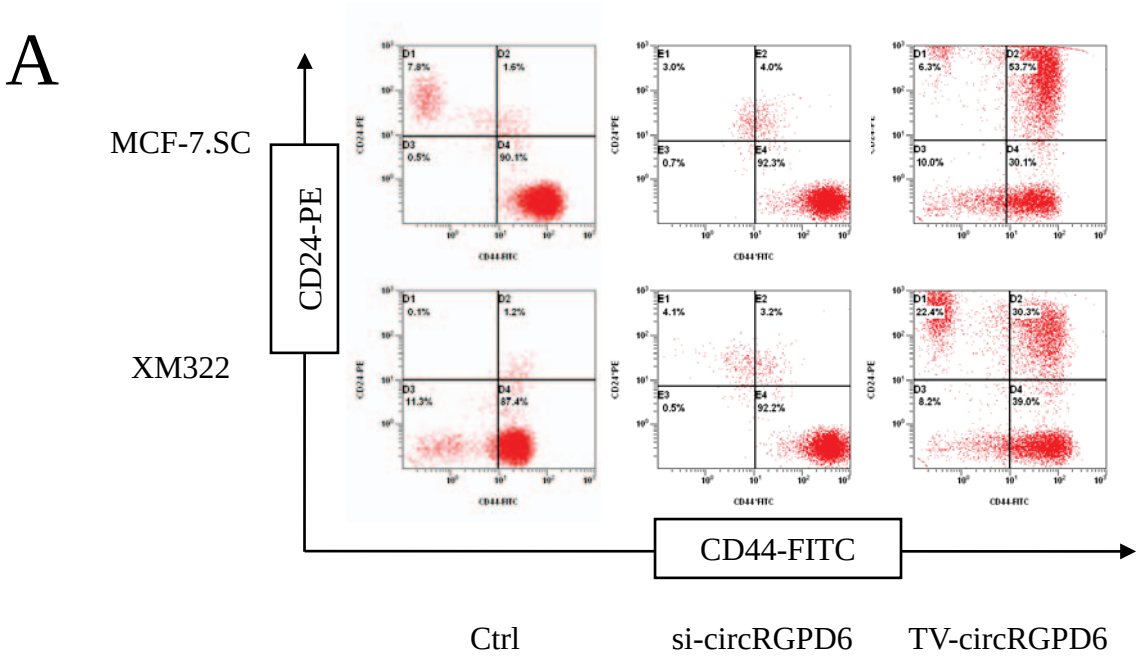

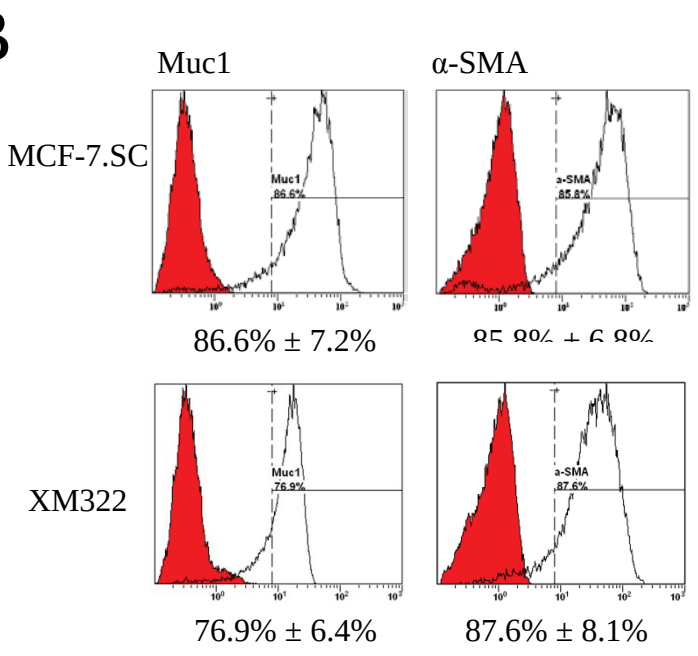

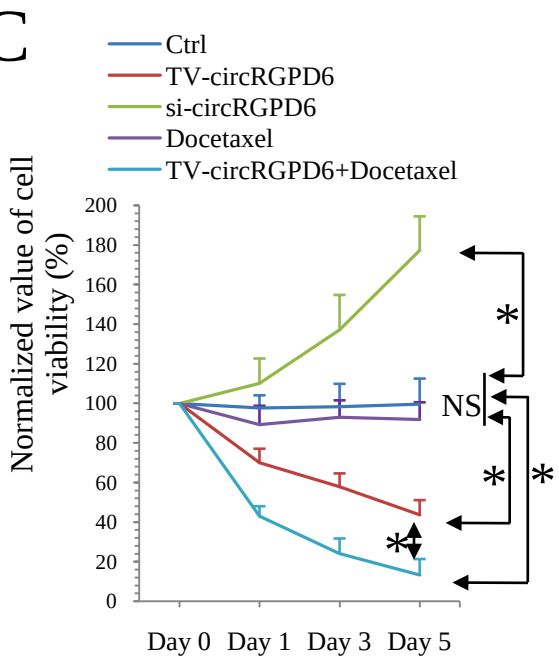

Figure S4. TV-circRGPD6 inhiblts tumor-initiating properties of BCSC *in vitro* (related to Figure 4). (A) Representative images of TV-circRGPD6 robustly decreasing the $CD44^{+}CD24^{-}$ subpopulation of MCF-7.SC and XM322. (B) TV-circRGPD6 enhanced the pluripotency in both MCF-7.SC and XM322. After differentiation, TV-circRGPD6 treated BCSC had increased Muc1-positive cells (Muc1-PE) accounted for approximately 80% (left panel) and increased α-SMA-PE positive cells accounted for approximately 85% (right panel). Peaks labeled in red represent isotype control. (C) MTT assays indicated that TV-circRGPD6 synergizes with docetaxel to eradicate XM322. Each experiment was repeated at least three times. * indicates P <0.05; NS: not significant. Statistical analyses were performed using multi-factor analysis of variance (univariate).

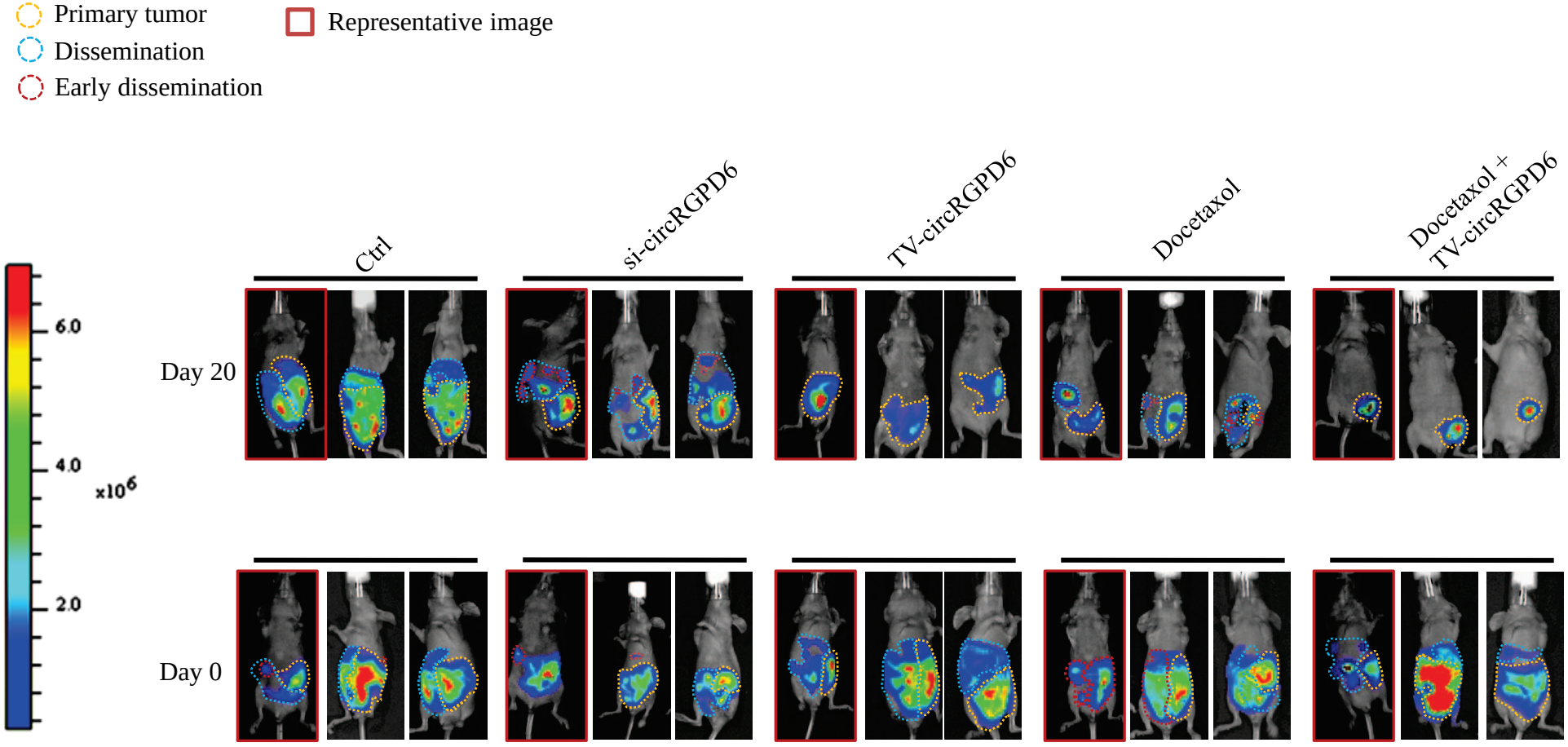

Figure S5. Photon signals of tumors in the XM322-bearing mice with Ctrl, si-circRGPD6, TV-circRGPD6, docetaxol alone, and Docetaxol plus TV-circRGPD6 (3 mice per group).

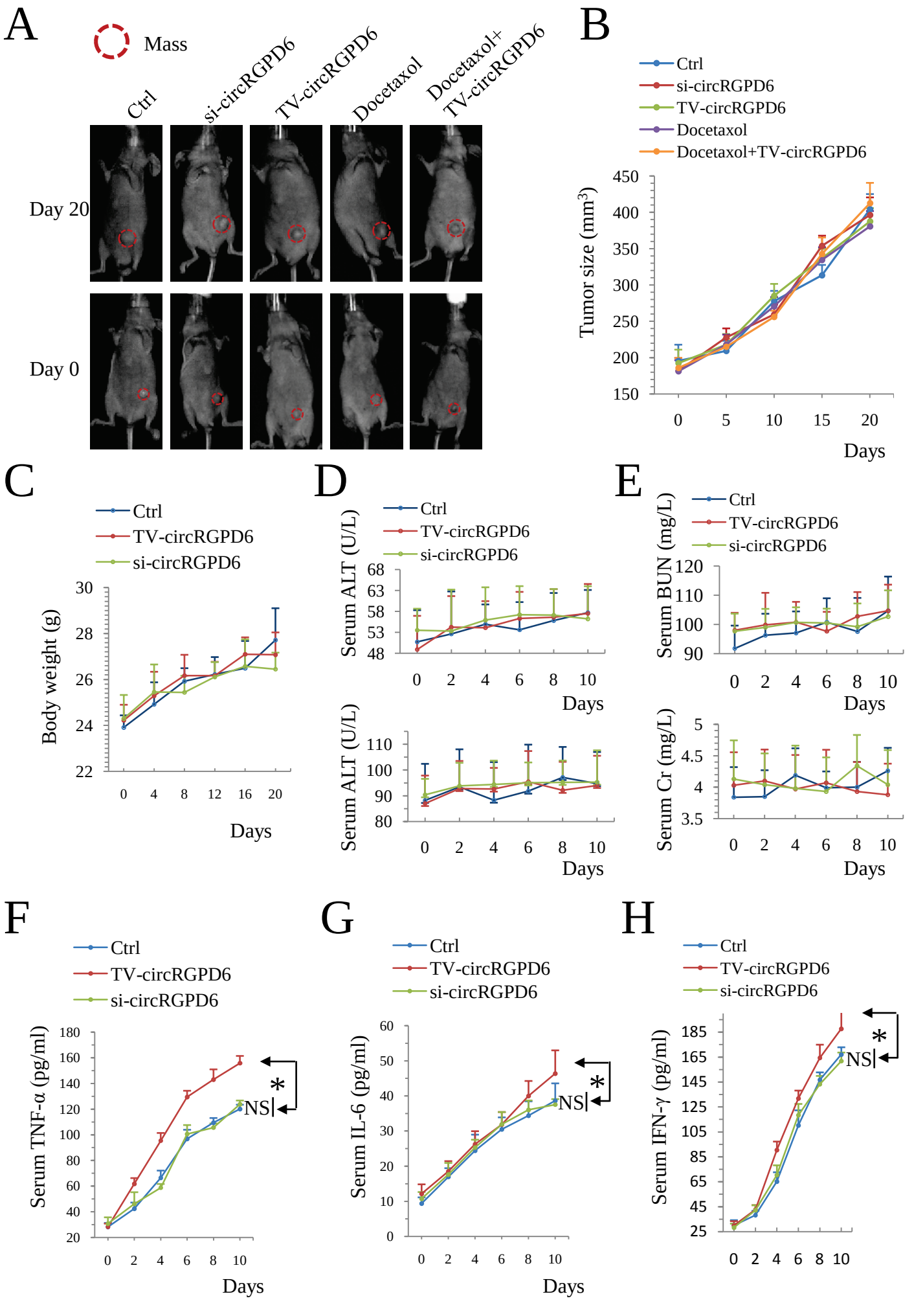
A
Mass
Ctrl
si-circRGPD6
TV-circRGPD6
Docetaxol
Docetaxol+ TV-circRGPD6
Day 20
Day 0
B
Ctrl
si-circRGPD6
TV-circRGPD6
Docetaxol
Docetaxol+TV-circRGPD6
Tumor size (mm3)
Days
C
Ctrl
TV-circRGPD6
si-circRGPD6
Body weight (g)
Days
D
Ctrl
TV-circRGPD6
si-circRGPD6
Serum ALT (U/L)
Days
Serum ALT (U/L)
Days
E
Ctrl
TV-circRGPD6
si-circRGPD6
Serum BUN (mg/L)
Days
Serum Cr (mg/L)
Days
F
Ctrl
TV-circRGPD6
si-circRGPD6
Serum TNF-α (pg/ml)
*
NS
Days
G
Ctrl
TV-circRGPD6
si-circRGPD6
Serum IL-6 (pg/ml)
*
NS
Days
H
Ctrl
TV-circRGPD6
si-circRGPD6
Serum IFN-γ (pg/ml)
*
NS

Figure S6. TV-circRGPD6 treatment for BCSC-bearing mice is well-tolerated *in vivo*. (A-B) Neither TV-circRGPD6 alone nor docetaxel alone plays an inhibitory effect on 184A1-bearing tumors *in vivo* (10 mice per group). Representative images (A) and statistical results (B) of xenografts growing in nude mice for 20 days after injection with 184A1. (C) Body weight of all nude mice in the experiment showed no significant change. (D) Serum ALT (upper panel) and AST (lower panel) of XM322-bearing mice with treatment of Ctrl, TV-circRGPD6 and si-circRGPD6 for 10 days. (E) Serum BUN (upper panel) and Cr (lower panel) of XM322-bearing mice with treatment of Ctrl, TV-circRGPD6 and si-circRGPD6 for 10 days. (F-H) Serum concentrations of TNF-α (F), IL-6 (G) and IFN-γ (H) of XM322-bearing tumors with treatment of Ctrl, TV-circRGPD6 and si-circRGPD6 for 10 days. Each experiment was repeated more than five times. * indicates P <0.05; NS: not significant

A

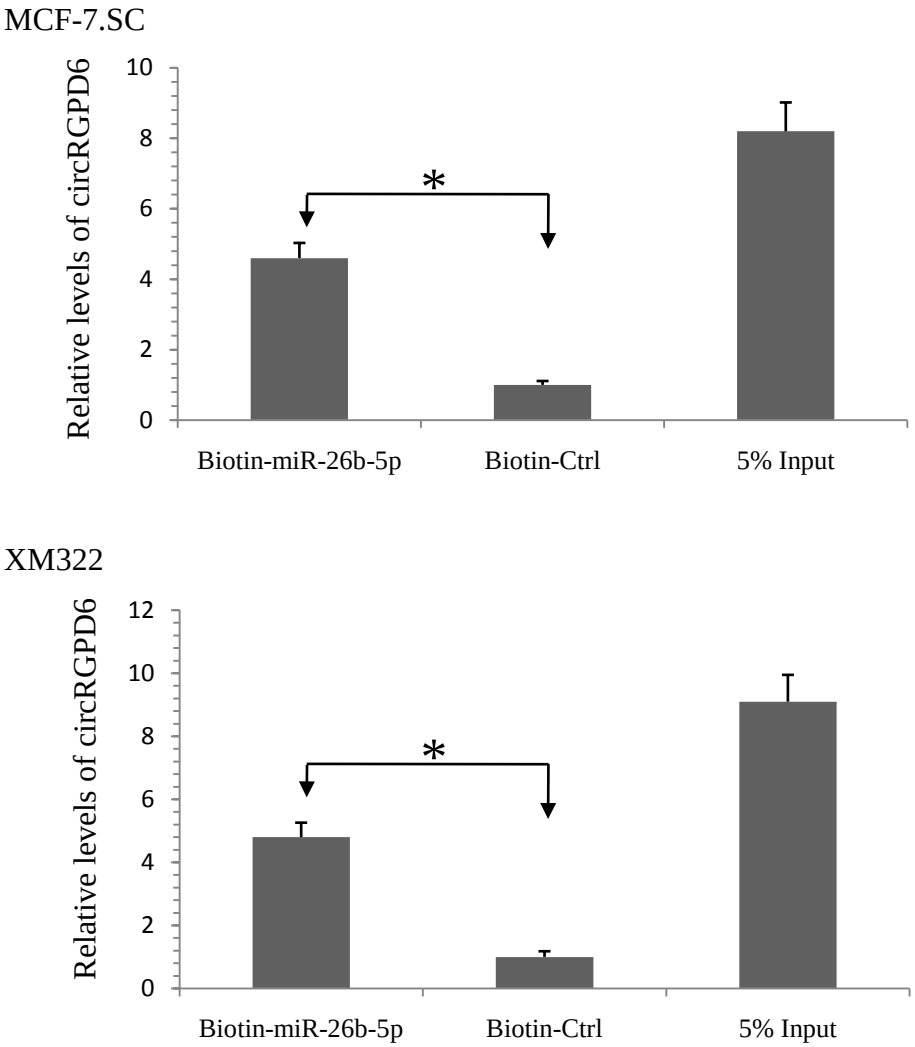

B

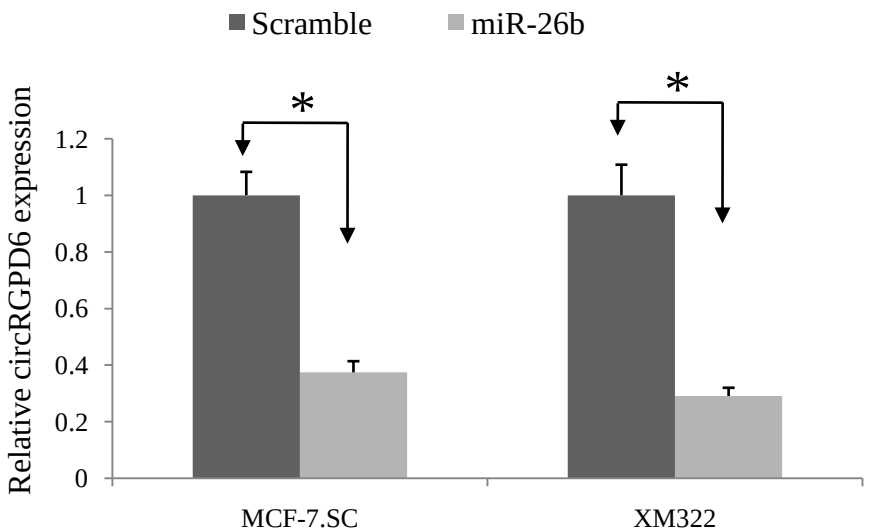

Figure S7. TV-circRGPD6 serves as a miRNA sponge for miR-26b (related to Figure 6). (A) We used a specific biotin-labelled miR-26b-5p probe to successfully capture circRGPD6 compared to the Ctrl group in MCF-7.SC (upper panel) and XM322 (lower panel). (B) qRT-PCR analyses of circRGPD6 expressions following transfection with a scrambled Ctrl, miR-26b mimics in MCF-7.SC and XM322. Statistical analysis was performed using the paired *t*-test.